Impact of high-risk conjunctions on Active Debris Removal target selection

Aleksander A. Lidtke, Hugh G. Lewis, Roberto Armellin

PII: S0273-1177(15)00535-9
DOI: http://dx.doi.org/10.1016/j.asr.2015.07.033
Reference: JASR 12366

To appear in: *Advances in Space Research*

Impact of high-risk conjunctions on Active Debris Removal target selection

Aleksander A. Lidtke[1,]

University of Southampton, Southampton, SO17 1BJ, UK

Hugh G. Lewis and Roberto Armellin[2]

University of Southampton, Southampton, SO17 1BJ, UK

Abstract

Space debris simulations show that if current space launches continue unchanged, spacecraft operations might become difficult in the congested space environment. It has been suggested that Active Debris Removal (ADR) might be necessary in order to prevent such a situation.

Selection of objects to be targeted by ADR is considered important because removal of non-relevant objects will unnecessarily increase the cost of ADR. One of the factors to be used in this ADR target selection is the collision probability accumulated by every object.

This paper shows the impact of high-probability conjunctions on the collision probability accumulated by individual objects as well as the probability of any collision occurring in orbit. Such conjunctions cannot be predicted far in advance and, consequently, not all the objects that will be involved in such dangerous conjunctions can be removed through ADR. Therefore, a debris remediation method that would address such events at short notice, and thus help prevent likely collisions, is suggested.

Keywords: active debris removal, target selection, just-in-time collision avoidance, collision probability, conjunction detection, orbital debris

Email addresses: `al11g09@soton.ac.uk` (Aleksander A. Lidtke), `H.G.Lewis@soton.ac.uk` `roberto.armellin@soton.ac.uk` (Hugh G. Lewis and Roberto Armellin)

[1]PhD student, Astronautics Research Group, University of Southampton, UK

[2]Lecturer, Astronautics Research Group, University of Southampton, UK

1. Introduction

It is a common belief that removing uncontrolled objects from Earth orbit is necessary to halt the increase of the debris population, most of which are expected to be fragments resulting from collisions (Liou, 2011). This phenomenon was indeed predicted in the 1970s (Kessler & Cour-Palais, 1978) but more attention has been paid to it recently as the self-exciting effect of collisions generating more debris and thus more collisions has been stipulated to be inevitable even if no future launches take place (Liou & Johnson, 2008). This has sparked world-wide interest in the development of technologies to stop this potential collision cascade.

At the time being it is difficult to assert whether such an "avalanche" of collisions will take place at all - the forecasts of the number of objects in orbit 200 years from now performed using the current debris environment models vary by as much as an order of magnitude (White & Lewis, 2014). However, there are other incentives to avoid collisions in orbit and to increase the sustainability of spaceflight, for example reducing the number of collision avoidance manoeuvres performed by the active satellites. This would effectively extend spacecraft lifetimes as they would have more propellant to conduct orbit maintenance.

It is argued by many authors that measures should be taken to address the potential growth of the number of debris objects in orbit (Liou, 2006, 2011; Pas et al., 2014; McKnight et al., 2012; Furuta et al., 2014). Several conceptually different approaches have been suggested over the years, ranging from reducing the number of debris added to the environment in the form of entire spacecraft or parts of thereof (mitigation) (Liou, 2006), active removal of derelict objects (Liou, 2011), or prevention of collisions between uncontrolled objects via just in time collision avoidance (JCA) (McKnight et al., 2012).

Two out of three mentioned approaches aimed at improving the sustainability of space activities require selection of objects that are to be targeted. Active Debris Removal (ADR) appears to be the most popular strategy (Liou, 2011; Pas et al., 2014; Furuta et al., 2014; McKnight et al., 2014) and it requires targets to be selected if not all the objects can be removed, e.g. due to financial or political constraints.

ADR is so popular because it ensures that mass is removed from orbit thus lowering the potential for future collisions. Due to the novelty of the technologies required to perform such removal missions and complexity of the necessary space systems, the cost of every such undertaking is expected to be high. Thus, reducing the number of removal missions by selecting the targets more appropriately becomes important.

A common option for the selection of ADR targets is ranking all the objects based on a single metric that reflects the risk a given object poses to the environment, which typically accounts for the chance of an object being involved in a collision (collision probability) with high severity (Liou, 2011; Rossi et al., 2014). Severity of collisions is said to be roughly proportional to mass because collisions of massive objects are likely to produce many new debris (Johnson et al., 2001). Performing Active Debris Removal of targets selected in this manner leads to several (at least 9.5 in a study by Liou & Johnson (2009)) objects that need to be removed to prevent a single collision, thus increasing the capital cost of ADR even further.

Removing more objects does not necessarily prevent more collisions (Liou & Johnson, 2009). This is because these targets are not necessarily the ones that *will* take part in dangerous conjunctions but rather the ones that are the *most likely* to have them. Therefore, in order to increase the confidence in the outcome of ADR using such target selection schemes, more objects need to be removed per year to reduce the probability of a collision taking place in orbit (Liou & Johnson, 2009).

Previous studies with DAMAGE (Debris Analysis and Monitoring Architecture to the Geosynchronous Environment, the evolutionary debris model of the University of Southampton) have hinted at the importance of individual conjunctions in the scope of the evolution of the entire debris population (Lewis & Lidtke, 2014). This work investigates this phenomenon in greater detail in order to show why statistical ADR target ranking metrics that ignore the individual conjunctions may not prevent all the orbital collisions if a limited number of ADR missions can be flown. It is stipulated that if these high-risk conjunctions can be predicted more accurately and addressed at short notice it is likely that more catastrophic collisions can be prevented.

This study investigates the behaviour in which collision probability, P_C, is accumulated by objects in orbit in fine spatial and temporal resolutions to examine the impact of individual high-risk conjunctions. Primarily the relative importance of different conjunctions, in terms of the collision probability that they contribute to the final collision probability of every object, was of interest. The method used to identify individual conjunctions is described first. The description of the methods used to estimate the collision probability for all the conjunction is given next. The relative importance of different conjunctions can be estimated without identifying and assessing the P_C of all the conjunctions to the best of our abilities, as long as the collision probabilities are not contrived and the frequency of conjunctions with high collision probabilities is similar to what takes place when using higher fidelity methods. Therefore, certain inaccuracies in the algorithms and the input data were acceptable because using the highest-accuracy propagators and ephemerides would increase the computational time required for the analysis. Wherever practical, however, the precision of the used numerical schemes etc. was kept high not to degrade the results further.

Once the method used to find and assess conjunctions is described, its application to the study of the debris environment is described. The results are presented, the limitations stemming from the employed method discussed, and the conclusions drawn.

2. Conjunction detection and assessment

In order to achieve the goals of this study a new debris simulation framework was developed. It uses a freeware implementation of the simplified general perturbations (SGP4) propagator (Kelso, 2013) together with Two-Line Element sets (TLEs) (Hoots & Roehrich, 1988). The predictions made with this propagator are only accurate to within several days but it allows the major perturbing forces on a satellite to be modelled while being computationally fast, which allows simulations of all the objects in orbit to be performed. TLEs are not provided with uncertainty information, therefore their covariance has to be estimated. However, these TLE uncertainty estimation methods provide only approximate accuracy of the orbital elements, not the actual covariances. Lastly, TLEs are officially said to be unsuitable for conjunction screenings. However, they do remain the only publicly available source of ephemerides. They were also used for operational collision avoidance performed by the European Space Agency (Flohrer et al., 2011) and other organisations that did not maintain their own catalogue of space objects before the US Strategic Command (USSTRATCOM) offered to issue conjunction warnings to spacecraft operators.

2.1. Conjunction detection

Conjunctions between all the objects in the public TLE catalogue have to be identified. A conjunction is defined as a time when centres of mass of two objects are within a specified distance from one another. This may not necessarily be the time when the collision probability between the two objects is the greatest if their attitude is accounted for, but this was ignored in this study.

Different distance thresholds in e.g. in-track or cross-track directions can also be used for conjunction detection in order to account for the fact that the position uncertainties are generally not the same in every direction (Alfano, 1994; Coppola & Woodburn, 1999) and so conjunctions with the same separation between centres of mass might have different collision probabilities. However, it was decided to account for this by setting the conjunction threshold distance high and equal in every direction, and accepting that certain conjunction geometries may result in very low collision probabilities with such a miss distance. Furthermore, conjunctions between more than two objects were treated as multiple conjunctions between pairs of objects.

Even with such a simple formulation of a conjunction the computational time required to identify them between all the objects in the public catalogue (14 917 objects had been observed in the 30 days preceding 7 Nov 2013 and their orbits were published via Space-Track (2013)) is significant. This raises the need to implement a number of pre-filters that discard pairs of objects that cannot have a conjunction based on simple and fast to evaluate flight dynamics principles before the more computationally-intensive range-based detection is executed.

A number of pre-filters have been developed to date, starting with the method by Hoots et al. (1984) as well as alternative approaches adopted by Khutorovsky et al. (1993), Healy (1995) and Rodriguez et al. (2002). New approaches are being developed, e.g. by Budianto-Ho (2014), but the objective of this work was not to contribute towards the development of such tools. Therefore, a set of traditional algorithms, based on the the "smart sieve"developed by Rodriguez et al. (2002), was decided upon. The details of how the pre-filters were implemented exactly and how the times of closest approach (TCA) were found are given in Lidtke et al. (2014).

2.2. Collision probability estimation

Once a conjunction has been identified the state vector uncertainties of both involved objects are propagated to the time of the closest approach.

The collision probability is computed by evaluating a multivariate integral of the probability density function of the relative position of the two objects involved in the conjunction over the volume swept out by their combined hard-body area. Different methods for evaluating this integral exist, but a classical one, where every conjunction is analysed in a B-plane frame of reference, which is a plane normal to the vector of the relative velocity between the two objects, was adopted here (Berend, 1999; Alfano, 2007; Chan, 2009). The B-plane was centred on the centre of mass of one of the objects, which was arbitrarily chosen because both objects are equally important in this study.

First of all, the adopted collision probability estimation approach assumes zero-mean normal distribution of the position uncertainty so that it can be accurately described by a covariance matrix. This makes the prediction made herein only approximate c.f. reality as no distribution in truly normal. Furthermore, even if the initial uncertainty is normally distributed and has zero mean it will only remain such for several a limited number of orbital revolutions under the influence of orbital mechanics (Vallado & Seago, 2009).

New collision probability estimation algorithms, free of many of the simplifying assumptions, are being developed (Morselli et al., 2015), but their computational time still remains significant (order of 0.1 s per conjunction at best). Using such algorithms would increase the computational time needed for the analyses done in this study beyond an order of days, thus making it infeasible to perform multiple analyses. Therefore, the simplifying assumptions were accepted. The excessive computational cost of using higher-fidelity algorithms also makes it impossible to quantify the errors associated with the simplifying assumptions, because a reference set of results cannot be obtained. Qualitative analysis of the errors associated with the collision probability estimation, and its possible impact on the conclusions of this paper, is given in section 4.

The position covariances of both objects are propagated to the time of the closest approach and rotated to the B-plane according to the algorithm given e.g. by Berend (1999). By assuming that the position errors of both objects are uncorrelated individual covariance matrices are added to form a single covariance matrix C. The velocity covariance is ignored as it has been found not to affect the collision probability significantly (Berend, 1999) and this was confirmed by Monte Carlo analyses of several exemplar conjunctions.

Rectilinear relative motion and time-invariant position uncertainties are assumed in the vicinity of the TCA thus allowing the covariance matrix to be projected onto the B-plane and reducing the number of dimensions of the problem from three to two (Berend, 1999; Chan, 2009). McKinley (2002) has shown that even for relative velocities of 0.013 km/s the rectilinear relative motion assumption resulted in collision probability estimates to be in the same order of magnitude as when this assumption was relieved. Moreover, Frigm & Rohrbaugh (2008) found that this assumption held in over 99% cases for both LEO and GEO satellites that they analysed. However, the number of conjunctions that would be found here was expected to be much higher due the number of objects in the catalogue as well as finding conjunctions between all the objects, not a limited number of operational spacecraft. This would mean that more conjunctions would be affected by this approximation, which could impact the conclusions. Therefore, conjunctions with relative velocity lower than 0.1 km/s were filtered out. This rejection threshold is 10 times higher than in (Frigm & Rohrbaugh, 2008) but the position uncertainties of the ephemerides used here might be larger and so the conjunction durations longer and hence more prone to errors caused by the rectilinear relative motion assumption.

Once projected onto the B-plane, the position covariance matrices are converted into a probability density function (PDF) of the relative position centred on one of the objects. The PDF is numerically integrated in the Cartesian coordinates of the B-plane inside a circle with radius equal to the combined radii of the two objects (collision radius) and centred on the other object. This integration can be made faster by expressing it as an infinite series of analytical terms (Chan, 2009). To correctly model the collision probability of very close conjunctions a simple numerical integration scheme (two-dimensional trapezium method (Press, 2002)) was used when the collision radius r was greater than 80% of the miss distance, the series expansion with 50 terms was used elsewhere.

2.2.1. Object physical size

TLEs come with no information as to the size of the associated objects and thus certain assumptions had to be made to enable the collision probability to be computed.

A database containing the physical radii of objects launched up to 2003 (up to catalogue number 28057), originally compiled by The Aerospace Corporation, was used to allow the collision radius to be computed for some conjunctions. For the remainder of the catalogue, statistical data from the MASTER reference population of 1 May 2009, which is the reference population used e.g. in the IADC studies, were used. An average radius for rocket bodies (R/B), payloads (P/L), mission-related objects (MRO), and debris (DEB) was computed. The standard deviation of every group was also found and the results are shown in Table 1.

Some of the MASTER object types can be directly linked to TLEs through three-line element sets that contain information about the type of certain objects in their common name fields. As the three-line element set catalogue does not distinguish mission-related objects, the data for this type of object were not directly utilised. Moreover, the three-line element set database contains many objects that are not classified as payloads, rocket bodies or debris. For these objects the average size of the entire MASTER 2009 (all four types of objects) population was used.

Table 1: Radii of the objects according to the their types (rocket bodies (R/B), payloads (P/L), mission-related objects (MRO), and debris (DEB)) as present in MASTER reference population of 1 May 2009 and discerned in Space-Track's Three-Line Element sets.

Object type	R/B	P/L	MRO	DEB	Other
MASTER Object ID	1	2	3	4	$1, 2, 3, and\ 4$
Average radius (m)	1.769	1.769	0.539	0.156	0.347
Standard deviation (m)	0.815	0.782	0.722	0.555	0.780

There are many small objects classified as debris or mission related objects, which means the average radius of those groups of objects is low. However, in both groups, objects much larger than the mean exist, which gives rise to large standard deviations of the samples. This signifies that using an average radius for every group of objects is a simplification. It was, however, necessary for the analysis described herein. More importantly, it was found to affect the overall collision probability of exemplar objects by no more than 12% when an average MASTER 2009 radius ± one standard deviation (or 10 cm when the standard deviation is greater than the mean) is used, as long as a database of the object sizes is utilised for the remaining objects.

2.3. Public catalogue covariance estimation and propagation

Two-line element sets are not provided with uncertainty information, which complicates collision probability estimation with this type of orbit information. This lack of covariance can be overcome e.g. by computing the collision probabilities using objects spatial densities (Dominguez-Gonzalez & Sanchez-Ortiz, 2014), estimating TLE uncertainty (Flohrer et al., 2008), or using other algorithms to estimate collision probability (Kessler, 1981). However, only estimating TLE uncertainty allows individual conjunctions to be resolved, therefore this approach is adopted here.

It has to be pointed out, however, that these TLE uncertainties, and the resulting collision probabilities, are only estimates. The collision probabilities computed using the estimated uncertainties will, however, be henceforth referred to as the true collision probability for brevity.

In order to quantify the impact of using estimated, not actual, TLE covariances the uncertainty of those ephemerides would need to be known so that a comparison could be made. Alternatively, a different set of ephemerides with covariance could be used and the two sets of conjunctions and their collision probabilities compared. However, neither TLE covariance nor different ephemerides are publicly available; therefore the impact of this assumption could not be quantified. The impact of using estimated TLE uncertainty on the results and the conclusions, which are drawn here, is discussed in Section 4.

A method to estimate the covariance of a TLE based on previous TLEs for the same object was developed by Osweiler (2006) and implemented in this work. All the historical TLEs spanning a period of 14 days from the epoch of the TLE used for conjunction detection were gathered and the position residuals were computed with respect to that most-recent TLE for every object. The covariance matrix was then computed from these residuals by treating them as state observations and assigning all of them equal weight (Osweiler, 2006). If fewer than five TLEs were available for a given object it would be discarded from the analysis entirely as covariance estimated with so few observations would be contrived.

Moreover, certain TLEs had to be ignored in case they were erroneous or a manoeuvre had been conducted by the spacecraft in the 14-day time window. In order to do this, specific orbital energies of all the TLEs from the two-week window for a given object were analysed and the TLEs whose energies were more than three standard deviations above the average were rejected (Patera, 2008).

2.3.1. Verification

A set of estimated TLE covariances for objects spanning 18 orbital regimes in the eccentricity-inclination-perigee altitude space was compared to the results obtained with the implemented algorithm. These objects have been selected by Krag et al. (2007) as a representative sample that categorises varying levels of accuracy of TLEs in different orbital regimes. An overview of the orbital regimes and the exemplar object in each is given in Table 2.

These reference data had been obtained by propagating the TLE state and generating pseudo-observations hence. Then orbit determination was performed on these simulated observations and the resulting orbit propagated numerically. Comparison of the numerically propagated states to the ones generated with the original TLE yielded covariance. This process is detailed in (Flohrer et al., 2008).

Clearly, inclination, perigee altitude and eccentricity are only some of the factors that affect orbit determination uncertainty. They also might not have as much impact as, for example, orbit maintenance being performed by some of the objects, their radar cross section, type of the object and alike (Kaya & Snow, 2000). Therefore, using other criteria to parametrise uncertainties of the TLEs could be more appropriate. However, the set of the exemplar objects from Table 2 was used to compare the accuracy of TLE uncertainty estimation for those objects only. The uncertainty of every TLE used in this study was estimated individually. Therefore, if the estimation algorithm is sufficiently accurate for the exemplar objects, it should also be for any other one. The only way to extend this verification would be to compare estimated TLE covariances for a more exhaustive number of different types of objects in the catalogue, but such data were not available.

The approach adopted here was applied to the exemplar objects from Table 2 at the epoch as close to the reference date (1 Jan 2008) as possible. The relative errors of the estimated to reference TLE position standard deviations in the radial, in-track, cross-track (RIC) reference frame are presented in Table 3.

Unfortunately, for objects 23100, 27763 and 20944 the epochs of the TLEs were different by 7, 3, and 1 years, respectively, with respect to the reference epoch. This is because the TLEs for the representative objects were not available on Space-Track (2013) in the desired period.

The epoch differences for objects 27763 and 20944 are less than 28% of the solar cycle and the $F10.7$ solar flux did not vary by more than 20 SFU (Vallado & Finkleman, 2014) between these epochs and the reference date. The orbit determination accuracy depends on the accuracy with which the drag coefficient can be estimated. Accuracy of the drag coefficient estimation depends on the solar activity (Pardini et al., 2006), meaning that the orbit

Table 2: Orbital regimes in the eccentricity-inclination-perigee altitude space, objects' catalogue numbers (SSCs), and number of Two Line Element sets used to validate the TLE covariance estimation approach.

	$e \leq 0.1$								
	$h_P \leq 800\,\mathrm{km}$			$800 < h_P \leq 25000\,\mathrm{km}$			$25000\,\mathrm{km} < h_P$		
	$i \leq 30^\circ$	$30^\circ < i \leq 60^\circ$	$60^\circ < i$	$i \leq 30^\circ$	$30^\circ < i \leq 60^\circ$	$60^\circ < i$	$i \leq 30^\circ$	$30^\circ < i \leq 60^\circ$	$60^\circ < i$
SSC	27783	23100	23940	22176	24320	23736	24435	24435	24435
No. TLEs	13	24	30	17	19	16	12	12	12
	$e > 0.1$								
	$h_P \leq 800\,\mathrm{km}$			$800 < h_P \leq 25000\,\mathrm{km}$			$25000\,\mathrm{km} < h_P$		
	$i \leq 30^\circ$	$30^\circ < i \leq 60^\circ$	$60^\circ < i$	$i \leq 30^\circ$	$30^\circ < i \leq 60^\circ$	$60^\circ < i$	$i \leq 30^\circ$	$30^\circ < i \leq 60^\circ$	$60^\circ < i$
SSC	21223	14900	27763	21966	21833	20944	14069	14069	14069
No. TLEs	14	11	21	12	7	17	7	7	7

determination accuracy depends on the solar activity. Therefore, it can be expected that the epoch differences for objects 27763 and 20944 did not affect the orbit determination accuracy and so the covariance estimated for them should be similar to the reference data.

For the object 23100, however, the difference in the $F10.7$ solar flux was more than 100 SFU (Vallado & Finkleman, 2014) and so the orbit determination accuracy could have been vastly different. Moreover, since autumn of 2012, the way in which at least some TLEs are generated has changed (Hejduk et at., 2013). This makes a direct comparison between the estimated and reference covariance for 23100 questionable, because both sets of data could have been generated using vastly different ephemerides.

The number of TLEs spanning the 14-day window, used to estimate the covariance of the most-recent TLE, was different for every object. For objects 23100, 27763 and 20944, however, similar numbers of TLEs were available, that is 24, 21, and 17, respectively. Therefore this factor should not influence the relative accuracy of the results.

The difference between the in-track standard deviation in the orbital regime of the object 23100 and the reference data was investigated further. A different object, 25112, located in the same orbital regime was investigated because TLEs were available for it close to the reference epoch (one day difference). 25112 is a satellite as opposed to a rocket body, therefore it most likely experiences different drag, but objects in this orbital regime typically have position uncertainties in the same order of magnitude (Flohrer et al., 2008). The results of this investigation, in the same form as in Table 3 to allow direct comparison between the two, are given in Table 4.

As in the case of eight out of 18 orbital regimes, over one order of magnitude difference in the in-track position standard deviation is present for object 25112. This discrepancy is considerably smaller than for object 23100, however, which may hint that part of the source of error for 23100 was the seven-year difference between the epochs at which the uncertainties were estimated.

The standard deviations of position uncertainties obtained with the adopted approach are typically in the same order of magnitude as the ones estimated using the more involved algorithm in (Flohrer et al., 2008). The biggest differences can be seen in the in-track direction. This is not surprising as the Keplerian dynamics will cause the largest dispersion of the sample objects in this direction.

This natural stretching of the position uncertainty in the in-track direction will be further amplified by the atmospheric drag that affects in-track positions of the objects. It is difficult to accurately represent such non-conservative forces analytically (Easthope, 2014). Therefore, the simplifications made in the SGP theory are expected to cause dispersion of the sample TLEs to be the greatest in this direction (Easthope, 2014; Kelso, 2007), thus resulting in even greater in-track position standard deviation. The effect of drag affecting the covariance estimation accuracy can be seen by observing that the in-track standard deviation estimation inaccuracies are the greatest at low altitudes.

3. Debris environment study

3.1. Description

The presented conjunction detection and collision probability estimation tools have been used to identify the conjunctions between all the objects in a snapshot of the public TLE catalogue from 7 Nov 2013 containing 14 917 objects. The analysis was performed for a period of 30 days and the conjunction threshold distance between centres of mass of the objects was set

Table 3: Relative errors of the estimated to reference TLE position standard deviations in every orbital regime in radial, in-track, cross-track (RIC) reference frame. Regimes where the estimated and reference standard deviations differ by one order of magnitude indicated with light grey, and by two with dark grey.

	$e \leq 0.1$								
	$h_P \leq 800\,\mathrm{km}$			$800 < h_P \leq 25000\,\mathrm{km}$			$25000\,\mathrm{km} < h_P$		
	$i \leq 30°$	$30° < i \leq 60°$	$60° < i$	$i \leq 30°$	$30° < i \leq 60°$	$60° < i$	$i \leq 30°$	$30° < i \leq 60°$	$60° < i$
R	0.90	9.02	1.63	-0.74	0.70	1.25	0.34	0.34	0.34
I	0.43	270.34	3.01	5.58	90.36	27.22	4.60	4.60	4.60
C	2.82	8.97	2.77	0.85	14.24	-0.54	-0.17	-0.17	-0.17
	$e > 0.1$								
	$h_P \leq 800\,\mathrm{km}$			$800 < h_P \leq 25000\,\mathrm{km}$			$25000\,\mathrm{km} < h_P$		
	$i \leq 30°$	$30° < i \leq 60°$	$60° < i$	$i \leq 30°$	$30° < i \leq 60°$	$60° < i$	$i \leq 30°$	$30° < i \leq 60°$	$60° < i$
R	-0.64	3.79	10.36	2.34	0.67	67.90	0.69	0.69	0.69
I	0.96	7.80	27.73	2.18	1.12	58.80	25.50	25.50	25.50
C	-0.48	-0.15	-0.38	-0.29	-0.06	2.05	-0.28	-0.28	-0.28

Table 4: Results, in the form of relative error of the estimated to reference standard deviations of position in the RIC frame, for object 25112 with perigee altitude lower than 800 km, inclination between 30 and 60 degrees, and eccentricity less than 0.1. Regimes where the estimated and reference standard deviations differ by one order of magnitude indicated with light grey, and by two with dark grey.

SSC	25112
No. TLEs	24
R	-0.39
I	34.04
C	6.98

to 20 km. This threshold distance means that the centres of mass of the objects will be separated by 3.2 to 326.0 position standard deviations estimated in section 2.3. Such a relatively high value guarantees that many conjunctions with relatively low collision probabilities (P_C) will be recorded and that a large spectrum of collision probabilities will be seen. This ensures that the impact of the high-P_C events will not be overestimated.

The period of 30 days was split into six five-day intervals to reduce the likelihood that the assumption of the orbit uncertainty being normally distributed will not be true. This period was chosen because it is quoted as the approximate duration after which the element set may be inaccurate enough to make tracking of the object difficult (Hejduk et at., 2013). The epochs of the snapshots, together with the number of objects in each, are given in Table 5. Note that the objects launched in the analysis period were ignored from the analysis for simplicity. This is not going to impact the conclusions because certain objects were not present in the snapshot from the 7 Nov 2013 anyway, e.g. because their ephemerides are classified.

Table 5: Dates of the TLE catalogue snapshots used in this study together with the number of objects in each.

Date of snapshot	Number of objects
7 Nov 2013	14 917
11 Nov 2013	14 909
16 Nov 2013	14 888
21 Nov 2013	14 867
26 Nov 2013	14 838
1 Dec 2013	14 777

For every object the accumulated collision probability, which is the probability that *any* of the conjunctions would result in a collision, was computed at all the epochs when the given object was involved in a conjunction. The cumulative collision probability for N conjunctions E_i, each with collision probability $P(E_i)$, was computed as:

$$P(\text{any out of N}) = 1 - P\left(\bigcap_{i=1}^{N} \neg E_i\right) = 1 - \prod_{i=1}^{N}(1 - P(E_i)). \tag{1}$$

Equation 1 assumes that the conjunctions are independent, which is to say that the collision probability and the outcome of one do not affect others. Clearly, if the objects do collide any subsequent conjunctions cannot take place, but this was accounted for when formulating Eq. 1. If a collision does not take place, subsequent conjunctions may have higher collision probability because, for example, the objects might be getting closer. This is caused by astrodynamics and not the statistical treatment of the problem, however. Therefore, the statistical independence assumption holds true. Such treatment of the accumulated collision probability ensures that the second axiom of probability (probability of any collision taking place and probability of no collision taking place sum to 1.0) is preserved, regardless of the number of conjunctions (DeGroot & Schervish, 2014).

The accumulated collision probabilities were also multiplied by the objects' respective masses. Doing so allows examining the criticality of every conjunction from the debris environment point of view (Liou, 2011) because such a figure can be thought of as risk of increasing the number of objects in the environment posed by a given conjunction.

Risk is often computed by multiplying the probability of an event times the severity of it, which in this case is roughly proportional to mass because destructions of heavy objects are likely to produce many new debris (Johnson et al., 2001). The term "criticality"will henceforth be used when referring to collision probability multiplied by mass of the object.

A database of the masses of objects in the public TLE catalogue, relating the Space Surveillance Catalog (SSC) number to mass of a given object was used in this study. It was compiled by working with the manufacturers and hence estimating the dry mass of the objects. The database contained the intact objects launched until April 2013. Not all the objects in the used TLE catalogue snapshots were present in the database, however. If this was the case, the given object was ignored from all the analyses where this property was used. All such objects were included in the samples that only used probability metrics, however.

If two objects, one with mass data present in the database and one without, took part in a conjunction, the accumulated criticality of the former was updated whereas criticality of the latter was not. This is because the objects in the population were analysed individually and such treatment of individual conjunctions ensured that the criticality accumulated by the objects with known mass estimates reflected all the conjunctions they took part in.

Objects were ranked in descending order of the final accumulated criticality or collision probability. The evolution of the accumulated collision probabilities and criticalities over time was investigated in detail for 20 top objects. The general behaviour of the complete samples of objects was also examined.

3.2. Results

Only the objects for which at least five TLEs were available to estimate the TLE covariance (13 931 out of 14 917 objects) were used in the analysis. A subset of these that also had mass data in the used database, mentioned in section 3.1 (8241 objects), was also used for analyses using criticality. According to Space-Track (2013), 165 objects decayed during the duration of the simulation and all the conjunctions involving these objects after their decay epochs were excluded from the results. The number of objects left in the analysis at different stages is summarised in Table 6. Also, 7144 conjunctions with relative velocities less than 0.1 km/s were filtered out. Finally, 3 138 538 conjunctions were recorded.

Table 6: Numbers of objects left in the analysis after different stages of filtering objects.

Property	Number of objects left in the sample
Original 7 Nov 2013 snapshot	14 917
More than 5 TLEs	13 931
With known mass	8241
With known radius	7806
Re-entered during simulation	165

3.2.1. Behaviour of the top objects

The Space Surveillance Catalog numbers (SSCs) and common names of the top-20 objects in the lists using collision probability and criticality are shown in Table 7.

Firstly, it can be noted that compositions of the two lists are largely different. When mass of the objects is taken into account all the debris, e.g. METEOR 2-5 DEB (36916), and relatively low-mass satellites, for example all Iridium satellites with masses of 556 kg, are moved away from the top of the lists. Including mass in the criticality index enables focusing on the conjunctions involving the heaviest objects that are likely to drive the evolution of the debris environment (McKnight et al., 2014). That said, the lighter objects should still be kept in the analysis as they could potentially cause breakups of the large derelicts if the collision energies are high enough (Johnson et al., 2001).

When criticality is examined instead of P_C alone, mass of the objects appears to dominate the composition of the target list, which leads to large-mass satellites like Envisat or SL-16 rocket bodies to be close to the top of the list. That said, many of the objects in the criticality-based list have relatively low masses. For example, IRS 1D (24971) has mass of 1250 kg, i.e. 16% of Envisat (7800 kg). Even METEOR 2-3, number two on the list, has much lower mass than the first object, i.e. 2750 kg. This points out that the collision probability accumulated by every object is also important as far as risk of generating new fragments is concerned.

Many of the objects with the highest criticalities presented in Table 7 are not often referred to as potential targets for ADR, unlike Envisat or SL-16 rocket bodies (McKnight et al., 2014). This means that, even if ADR has already been performed on certain satellites, those objects would still accumulate high collision probability and thus, potentially, be involved in collisions. This situation was caused by the fact that some of the objects in Table 7 do not have a large cross-sectional area, large mass, or are not located in densely populated orbital regimes. Therefore, they are not found to be involved in many dangerous conjunctions in space debris simulations and so do not attract attention as potential ADR targets.

One of the reasons why objects that are not commonly referred to as likely objects to be removed through ADR made it to the target lists was the fact that they had conjunctions with relatively high individual collision probabilities. Table 8 shows how much the conjunction with the highest

Table 7: Catalogue numbers and common names of the six objects with the highest P_C and true criticality at the end of the simulation.

Index	P_C	Criticality
1	27386 ENVISAT	27386 ENVISAT
2	36916 METEOR 2-5 DEB	10514 METEOR 2-3
3	10514 METEOR 2-3	25400 SL-16 R/B
4	27450 IRIDIUM 97	14452 METEOR 2-10
5	14452 METEOR 2-10	28057 CBERS 2
6	28057 CBERS 2	25260 SPOT 4
7	25468 IRIDIUM 81	23705 SL-16 R/B
8	24971 IRS 1D	24971 IRS 1D
9	25285 IRIDIUM 62	25979 ARIANE 40 R/B
10	24945 IRIDIUM 32	22285 SL-16 R/B
11	25528 IRIDIUM 86	26070 SL-16 R/B
12	25042 IRIDIUM 39	19531 NOAA 11
13	24792 IRIDIUM 8	21397 OKEAN 3
14	24968 IRIDIUM 37	22803 SL-16 R/B
15	25577 IRIDIUM 20	22566 SL-16 R/B
16	25274 IRIDIUM 58	23657 SICH 1
17	24795 IRIDIUM 5	27450 IRIDIUM 97
18	25171 IRIDIUM 54	13272 SL-14 R/B
19	25287 IRIDIUM 64	23608 ARIANE 40+3 R/B
20	25531 IRIDIUM 83	20436 SPOT 2

criticality recorded for every of the top-20 objects contributed to the final criticality of that object. A single conjunction, involving ARIANE 40+3 R/B (23608) and SL-14 R/B (13272), gave rise to 50.11 and 37.54% of the criticality accumulated by those objects over one month, i.e. nearly as much as all the remaining conjunctions. Therefore, it is this conjunction that effectively placed those objects in their respective positions on the target list. Contributions greater than 10% can be observed for four more out of the 20 objects with the highest criticalities. This can also be seen on the P_C-based list, where a single conjunction contributed 10% or more to the final value accumulated by four objects.

The conjunction of ARIANE 40+3 R/B and SL-14 R/B took place 58 and 81 hours after the epochs of their TLEs. Due to this relatively low prediction time, the orbit uncertainties had not grown sufficiently to dilute the P_C of this conjunction. This indicates that the time, over which such high-P_C conjunctions can be forecast, is limited. The longer the prediction interval, the larger the orbit uncertainty and so the lower the collision probability of all the conjunctions.

3.2.2. Importance of individual conjunctions

Single events with the highest collision probabilities gave rise to a similar portion of the collision probabilities and criticalities accumulated by top-20 objects as the rest of the conjunctions those objects were involved in. This was observed when examining the objects with the highest final P_C or criticality, where e.g. one event out of 461 conjunctions dominated the final accumulated collision probability and criticality of ARIANE 40+3 R/B (23608).

The percent contribution of the event with the highest recorded criticality to the final criticality accumulated over 30 days was computed for all the objects. A histogram showing the cumulative fraction of the population where a single event contributed a given percentage to the final accumulated criticality is shown in Fig. 1.

Conjunctions with the highest collision probability contributed at least 10% to the final criticality for 27.8% of the objects. A similar trend is also exhibited by the top 20 objects where, for 6 out of 20 top objects, particular events added 10% or more to the final accumulated criticalities. However, contribution higher than 40% was only observed for one of the top-20 objects, whereas for the entire population a single event contributed at least 90% to the final P_C for 3.4% of the objects.

Table 8: Contributions of the conjunctions with highest P_C to the final collision probability and criticality accumulated by objects from Table 7.

Index	P_C	Criticality
1	9.50%	9.50%
2	19.75%	3.52%
3	3.52%	5.07%
4	3.69%	2.22%
5	2.22%	2.52%
6	2.52%	13.93%
7	4.25%	1.66%
8	4.49%	4.49%
9	26.93%	16.46%
10	7.82%	2.47%
11	31.69%	1.29%
12	6.20%	9.83%
13	7.90%	11.54%
14	23.52%	1.44%
15	5.34%	1.28%
16	6.92%	15.61%
17	5.50%	3.69%
18	6.06%	37.54%
19	9.71%	50.11%
20	9.67%	3.33%

The probability of any collision taking place in orbit over the one-month time window was also computed. Figure 2 shows how this probability depends on the number of conjunctions. The conjunctions were sorted in ascending criticality order, i.e. the ones that contribute the most to the final accumulated value are included last. When computing this criticality, mass of both objects involved in a conjunction was used. It can be noted that half of the collision risk was caused by 200 conjunctions out of 3 073 330, i.e. only 0.0065% of the events.

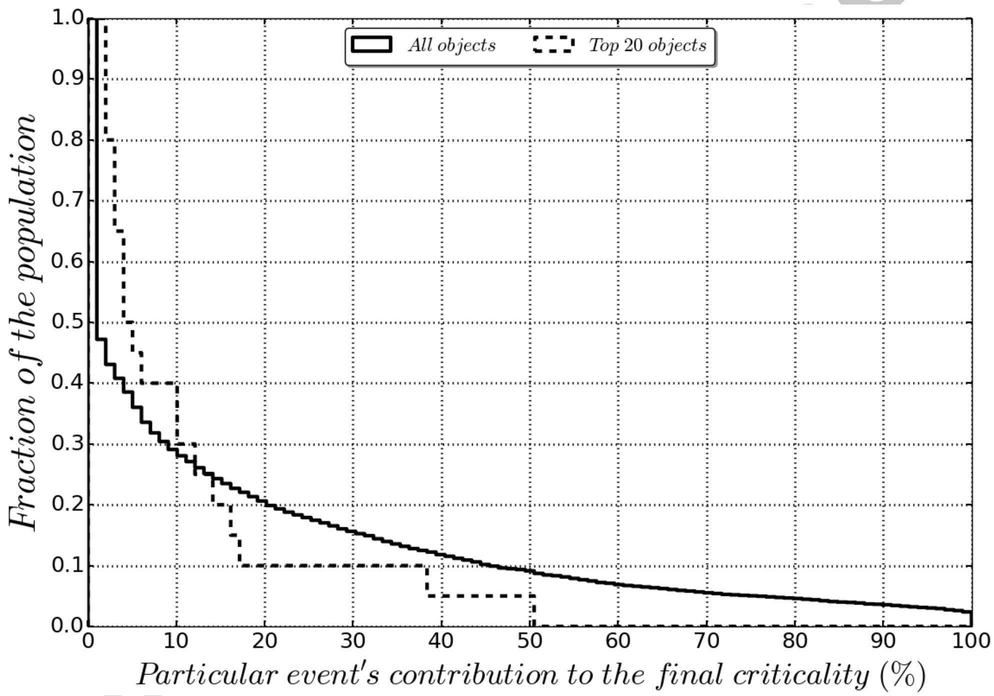

Figure 1: Cumulative histogram showing the fraction of the sample for which the highest criticality events contributed a given percentage or more to the final accumulated criticality. Objects with zero mass, no mass data, or with too few TLEs were excluded. Normalised with respect to the total number of objects in the sample (20 top objects or the entire population of 8241 objects).

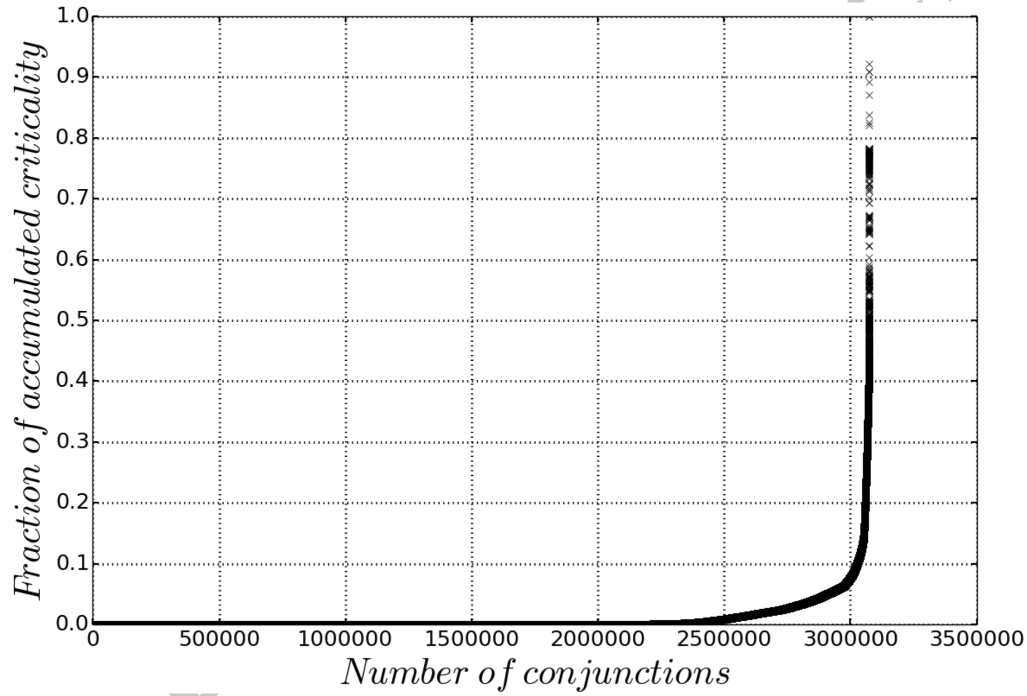

Figure 2: Evolution of the criticality accumulated by all the conjunctions in the entire debris environment. Conjunctions sorted in ascending P_C order. 50% of the criticality was due to 200 conjunctions out of 3 073 330 (0.0065%).

4. Discussion

Several simplifications were made when generating the data on which the findings of this work are based. This was done to reduce the computational time needed for the analysis and to make it feasible given the computational resources that were available.

These simplifications include e.g. using approximate object masses and sizes, ignoring their attitude, estimating uncertainty of the ephemerides, or making several simplifying assumptions when computing the collision probabilities of individual conjunctions. There are several ways in which these could have affected the collision probabilities of the objects and the related criticalities.

Missing potentially very close conjunctions or incorrectly computing collision probabilities due to interpolation errors would alter the collision probabilities of individual objects. Using a physical radius from the database for certain objects but not for the others could render the collision probabilities of the objects with assumed radius different to what they would be when using their actual size. On the other hand, using the database of sizes ensures that the objects much larger than others of the same type, and hence average MASTER 2009 radius, will experience higher collision probabilities as they would in reality. Furthermore, ignoring the attitude of the objects and other simplifying assumptions in the collision probability estimation algorithms mean that different collision probabilities of individual conjunctions could have been found had higher-fidelity algorithms been used.

However, the point of this work was not to examine the conjunctions that took place in reality as accurately as possible. The conjunctions were detected using a set of actual objects to provide a real-life example of a set of the possible events that *could* occur in reality. Despite the assumptions and simplifications that were made, a large spectrum of collision probabilities was found for every object. For the satellite with the highest contribution of a single conjunction to the final accumulated collision probability out of the top-20, i.e. IRIDIUM 86, the P_C of individual conjunctions varied from 2.95×10^{-234} to 6.31×10^{-7}. Collision probabilities of all the conjunctions were inversely proportional to the miss distance, scaled with size of the objects etc. as they would when using higher-fidelity methods and ephemerides. This means that the set of *exemplar* conjunction geometries found with the TLE catalogue snapshot provided a corresponding set of *exemplar* collision probabilities and the events with high collision probability were as infrequent as the ones with very low miss distance.

Such high collision probability conjunctions do take place when using higher fidelity ephemerides and algorithms, which leads to conjunction screenings being routinely performed for operational spacecraft (Flohrer et al., 2009). The existence of such events is not an artefact resulting from the ephemerides or the assumed object sizes, for example.

It cannot be guaranteed that all the conjunctions of every object were affected by the simplifications of this study in the same manner, meaning that the contributions of the highest-probability events to the final collision probabilities may not be exactly what they would be if using the highest-fidelity input data and algorithms. However, this does not undermine the finding that the frequency at which such high-probability events occur is low (one in over a thousand for the 20 objects with the highest P_C, sometimes as many as 2120). Neither does this change the finding that these relatively infrequent, high-probability events dominate the others, which have lower collision probabilities, as far as final accumulated collision probability is concerned. Similar behaviour has also been found by McKnight et al. (2014). Lastly, it was shown in section 2.3 that the TLE covariances tend to be over-, rather than under-estimated. Therefore, actual collision probabilities of high-P_C conjunctions, and so their relative importances, might be higher than found here if more precise ephemerides are used.

However, the simplifications made to obtain the results presented herein mean that the identified objects were not necessarily the ones most likely to be involved in a collision in the the analysed time period. This is especially true because only several events had the largest contribution to the formulation of these lists and the collision probabilities of these events were affected by the assumptions made here. Conjunctions with higher collision probabilities could have taken place and these could not have been identified here and, consequently, objects involved in those could not have been included in the target lists.

Moreover, the fact that the TLE catalogue obtained at only one epoch was analysed means that the identified objects may not be the ones with the highest probability of being involved in a collision in the long term. In fact, the most risky objects could not have been present in the analysis if their ephemerides are not part of the "public catalogue" available on Space-Track (2013), which is to say they are classified.

Therefore, the exact composition of the lists of objects with the highest collision risk cannot be relied upon. But what remains valid, despite the simplifications that were made in this study, is the impact of the highest-probability conjunctions on the final accumulated collision probabilities of the objects.

Predicting the objects that will be involved in those conjunctions would require methods with fidelity higher than the ones used here, however. It is expected that variations in atmospheric density will affect collision probabilities of the conjunctions, and ultimately lead to collisions that cannot be forecast far in advance. This is due to, for example, the fact that the short-timescale changes in the solar activity are inherently unpredictable and those will affect the atmospheric density and, consequently, also the positions of the objects.

Even with the highest-accuracy ephemerides, propagators, force models etc., it is not expected that conjunctions could be forecast for more than several days or at most a few weeks ahead. This creates a need for a system that would address potential collisions at short notice when the conjunctions can still be accurately predicted.

A debris remediation architecture that operated with such short lead times would differ from what is currently being proposed in the field of space debris remediation. Perhaps even a ground-based laser (Mason et al., 2011) or an air-launched "nudger"(McKnight et al., 2012) system would suffice to prevent the most-dangerous conjunctions. This can be achieved by exerting a force on the involved objects and increasing their miss distance, and thus reducing the collision probability.

Certainly the longer the period over which the collisions can be accurately forecast, the easier it would be to implement a mission to prevent them. This can only be achieved if improvements in Space Surveillance and Tracking (SST) systems, propagators and force models are made. Nonetheless, extremely rapid deployments of such debris remediation missions (order of days) will need to take place if such an approach to debris remediation is followed.

Of course, all debris remediation strategies that do not remove the collision risk entirely, by removal of all the objects, might not prevent all the collisions. But, unlike a statistical target selection approach, a collision prevention method could use the most accurate collision forecasts and hence could potentially address the most likely collisions that cannot be reliably forecast far in advance. Evolution of the collision probability, encounter geometry, object details, and potential impact of a collision could also be taken into consideration. Furthermore, an approach that addressed individual conjunctions, rather than statistically-important objects, would allow an accepted risk threshold to be set. This would enable the residual risk due to some of the conjunctions being ignored to be quantified. Being able to set such a threshold would enable the benefit of reducing the residual risk to be traded off against the cost of preventing more collisions.

Many of the objects that are commonly referred to as the most likely candidates to be removed, e.g. SL-16 rocket bodies or Envisat (McKnight et al., 2012), were found amongst the ones with the highest criticality. This is because these objects have relatively high masses, are large in size and are the most likely to be involved in dangerous conjunctions because they are located in densely populated orbital regimes. However, other objects were also identified amongst the ones with the highest accumulated collision probabilities, e.g. ARIANE 40+3 R/B (23608), CBERS 2 or METEOR 2-3.

It is hence recommended that a discussion about the fundamental approach to space debris remediation be initiated and an *ad hoc* architecture, which prevents the collisions when they can be accurately forecast (McKnight et al., 2012), be evaluated alongside popular approaches that remove mass from the environment using statistical target selection schemes. This is primarily because, if not all or most of the derelict objects are removed, collisions may still occur despite the efforts to prevent them by removal of statistically important objects.

5. Conclusions

Particular conjunctions with high P_C were shown to contribute more to the collision probability accumulated by certain individual objects in a short time window than the remaining conjunctions with lower collision probabilities. This was observed primarily for the objects with the highest maximum collision probabilities in the given time window, but also for the remaining objects in the sample - for 27.8% of the objects a single event contributed 10% or more to the final accumulated maximum criticality of the object. Similarly, half of the probability of any collision taking place in the analysed month could be attributed to 200 conjunctions.

The ability to predict such events with high collision probability was also discussed. It is, however, impossible to draw binding conclusions regarding the currently achievable forecast durations given the relatively low fidelity of the data and propagators used in this study. Regardless of the ephemerides used, conjunctions cannot be reliably forecast more than several days or at most weeks ahead. This is, for example, due to the fact that the daily solar activity can lead to unpredictable changes in the atmospheric density, and thus positions of the objects and conjunction details. This means that conjunctions with high-P_C will occur and significantly change the collision probabilities of individual objects, thus redefining the most risky objects in a given time interval.

Moreover, those high-P_C events can involve objects that are not large or located in densely populated orbital regimes and thus are not often quoted as "risky" in the context of increasing the number of space debris, for example ARIANE 40+3 R/B (23608) or CBERS 2. This is because these objects do not take part in many conjunctions on a daily basis or in simulations. This means that, unless all the derelicts are removed from orbit, collisions might happen despite the efforts to prevent them through active removal of objects likely to have many conjunctions. The only alternative to removal of all the objects seems to be prevention of collisions in an *ad hoc* fashion, when they can be forecast.

However, this study found that many objects, which take part in dangerous conjunctions, are the ones with large cross section areas and located in densely populated orbital regimes, i.e. will be found dangerous when examining long-term collision probabilities of the objects. Permanently removing those might be a lot more cost-effective than preventing the conjunctions they take part in. Therefore, a mixed approach where ADR is used to remove the objects that will take part in many conjunctions, and *ad hoc* collision prevention to ensure that the unpredictable collisions are avoided, is recommended to contain the number of objects in Earth orbit. Otherwise the unpredictable collisions may thwart any debris remediation efforts.

6. Acknowledgements

The authors are grateful for the comments of the anonymous reviewers that greatly improved the quality of this work.

The authors acknowledge the use of the IRIDIS High Performance Computing Facility, and associated support services at the University of Southampton, in the completion of this work.

Big thanks to J.C. Liou for an interesting discussion about the importance of removal of mass from the debris environment during the 3rd European Workshop of Space Debris Modelling and Remediation.

The authors would like to thank the ESA Space Debris office for allowing them to use the MASTER 2009 reference population. Dedicated thanks go to Holger Krag and Tim Flohrer for their extremely valuable feedback and discussion regarding operational collision avoidance, help in validating the collision probability algorithms, and provision of the set of estimated TLE covariances.

Sincere thanks to David Vallado for distribution of the SGP4 propagator code, without which this research would never be possible in the timeframe available.

The authors would also like to express their gratitude to T.S. Kelso for useful comments regarding the collision probability, maintaining the CelesTrak website, and provision of the objects' physical radii database.

The authors would also like to acknowledge the use of AGI's Systems Toolkit in the verification process of the developed simulation framework.

Finally, the authors would like to express their gratitude to Darren McKnight for provision of the objects' masses database and important comments regarding this work.

7. References

References

Alarcon Rodriguez, J.R., Martinez Fadrique, F., & Klinkrad, H., Collision risk assessment with a 'smart sieve' method, Joint ESA-NASA Space-Flight Safety Conference, Noordwijk, the Netherlands, ESA SP-486, 2002.

Alfano, S., Determining Satellite Close Approaches, Part II, The Journal of the Astronautical Sciences, 42, 143-152, 1994.

Alfano, S., Review of Conjunction Probability Methods for Short-term Encounters, AAS/AIAA Space Flight Mechanics Meeting, Sedona, AZ, USA, 2007.

Berend, N., Estimation of the probability of collision between two catalogued orbiting objects, Adv. Space Res., 23, 243-247, 1999.

Budianto-Ho, I., Scalable Conjunction Processing Using Spatialotemporally Indexed Ephemeris Data, Advanced Maui Optical and Space Surveillance Technologies Conference, Wailea, HI, USA, 2014.

Chan, K., International Space Station Collision Probability, The Aerospace Corporation, Chantilly, VA, USA, 2009.

Coppola, V., & Woodburn, J., Determination of Close Approaches Based on Ellipsoidal Threat Volumes, Advances in the Astronautical Sciences, 102, 1013-1024, 1999.

DeGroot, M.H., & Schervish, M.J., Probability and Statistics, Fourth Edition, Pearson Education Limited, Harlow, UK, 2014.

Dominguez-Gonzalez, R., & Sanchez-Ortiz, N., Classification of TLE-catalogue objects in regard to their long-term collision probabilities, 3rd workshop of Space Debris Remediation, Paris, France, 2014.

Easthope, P.F., Examination of SGP4 along-track errors for initially circular orbits, IMA Journal of Applied Mathematics, on line, 115, 2014.

Flohrer, T., Krag, H., & Klinkrad, H., Assessment and Categorization of TLE Orbit Errors for the US SSN Catalogue, Advanced Maui Optical and Space Surveillance Technologies Conference, Wailea, HI, USA, 2008.

Flohrer, T., Krag, H., & Klinkrad, H., ESA's process for the identification and assessment of high-risk conjunction events, Adv. Space Res., 44, 355-363, 2009.

Flohrer, T., Klinkrad, H., Krag, H., Bastida Virgili, B., & Merz, K., Operational Collision Avoidance for LEO Satellites at ESA, Proceedings of the 28th International Symposium on Space Technology and Science, Okinawa, Japan, 2011.

Frigm, R.C. & Rohrbaugh, D., Relative Velocity as a Metric for Probability of Collision Calculations, Proceedings of the 59th International Astronautical Congress, Glasgow, Scotland, IAC-08-A6.2.5, 2008.

Furuta, S., Hanada, T., Fujita, K., & Takezono, K., Discussion on the Necessity of Orbital Debris Removal in the Geostationary Region, 65th International Astronautical Congress, Toronto, Canada, IAC-14.A6.2.2, 2014.

Healy, L.M., Close Conjunction Detection on Parallel Computer, Journal of Guidance, Control, and Dynamics, 18, 824-829, 1995.

Hejduk, M.D., Casali, S.J., Cappellucci, D.A., Ericson, N.L., & Snow, D.A., A Catalog-Wide Implementation of General Perturbations Orbit Determination Extrapolated From Higher Order Orbital Theory Solutions, 23rd AAS/AIAA Spaceflight Mechanics Conference, Kauai, HI, USA, 2013.

Hoots, F.R., Crawford, L.L., & Roehrich, R.L., An Analytic Method to Determine Future Close Approaches, Celestial Mechanics, 102, 143-158, 1984.

Hoots, F.R., & Roehrich, R.L., SPACETRACK REPORT NO. 3 Models for Propagation of NORAD Element Sets, 1988.

JFCC SPACE, Space-Track, Last accessed: 11 August 2014, URL: `www.space-track.org`, 2013.

Johnson, N.L., Krisko, P.H., Liou, J.C., & Anz-Meador, P.D., NASA's new breakup model of evolve 4.0, Adv. Space Res., 28, 1377-1384, 2001.

Kaya, D.A. & Snow, D.E., Element set accuracy assessment, Advances in the Astronautical Sciences, 103, Part II, 1937-1946, 2000.

Kelso, T.S., Validation of SGP4 and IS-GPS-200D Against GPS Precision Ephemerides, 17th AAS/AIAA Spaceflight Mechanics Conference, Sedona, AZ, USA, 2007.

Kelso, T.S., Satellite Tracking Software, Last accessed: 26 April 2014, URL: `www.celestrak.com/software/tskelso-sw.asp`, 2000.

Kessler, D.J., & B.G. Cour-Palais, Collision frequency of artificial satellites: The creation of a debris belt, J. Geophys. Res., 83 (A6), 2637-2646, 1978.

Kessler, D., Derivation of the Collision Probability between Orbiting Objects: The Lifetimes of Jupiter's Outer Moons, Icarus, 48, 39-48, 1981.

Khutorovsky, Z.N., Boikov, V., & Kamensky, S.Y., Direct method for the analysis of collision probability of artificial space objects in LEO: techniques, results and applications, First European Conference on Space Debris, Darmstadt, Germany, ESA SD-01, 1993.

Krag, H., Klinkrad, H., & Alarcon-Rodriguez, J.R., Assessment of Orbit Uncertainties for Collision Risk Predictions at ESA, Second IAASS conference "Space safety in a global world", Chicago, IL, USA, 2007.

Lewis, H.G., & Lidtke, A., A Collision Conundrum: Investigation of Envisat Collision Hazard, 32nd Inter-Agency Space Debris Coordination Committee Meeting, Beijing, China, 2014.

Lidtke, A.A., Lewis, H.G. & Armellin, R., A Deterministic Approach to Active Debris Removal Target Selection, Advanced Maui Optical and Space Surveillance Technologies Conference, Wailea, HI, USA, 2014.

Liou, J.C., Collision activities in the future orbital debris environment, Adv. Space Res., 38, 2102-2106, 2006.

Liou, J.C., Johnson, N.L., Instability of the present LEO satellite populations, Adv. Space Res., 41, 1046-1053, 2008.

Liou, J.C., Johnson, N.L., A sensitivity study of the effectiveness of active debris removal in LEO, Acta Astronautica, 64, 236-243, 2009.

Liou, J.C., An active debris removal parametric study for LEO environment remediation, Adv. Space Res., 47, 1865-1876, 2011.

Mason, J., Stupl, J., Marshall, W. & Levit, C., Orbital debris-debris collision avoidance, Adv. Space Res., 48, 1643-1655, 2011.

McKinley, D., Development of a Nonlinear Probability of Collision Tool, AIAA/AAS Astrodynamics Specialist Conference, Monterey, CA, USA, AIAA 02-4744, 2002.

McKnight, D., DiPentino, F., Musekamp, D., & Dingman, P., System Engineering Analysis of Derelict Collision Prevention Options, 63rd International Astronautical Congress, Naples, Italy, IAC-12.A6.5.2, 2012.

McKnight, D., DiPentino, F., & Knowles, S., Massive Collisions in LEO - A Catalyst to Initiate ADR, 65th International Astronautical Congress, Toronto, Canada, IAC-14.A6.2.1, 2014.

Morselli, A., Armellin, R., Di Lizia, P., & Bernelli Zazzera, F., A high order method for orbital conjunctions analysis: Monte Carlo collision probability computation, Adv. Space Res., 55, 311-333, 2015.

Osweiler, V.P., Covariance estimation and autocorrelation of NORAD two-line element sets, Air Fore Institute of Technology, Wright-Patterson Air Force Base, OH, USA, 2006.

Pardini, C., Kent Tobiska, W., & Anselmo, L., Analysis of the orbital decay of spherical satellites using different solar flux proxies and atmospheric density models, Adv. Space Res., 37, 392-400, 2006.

Pas, N., Lousada, J., Terhes, C., Bernabeu, M., & Bauer, W., Target selection and comparison of mission design for space debris removal by DLRs advanced study group, Acta Astronautica, 102, 241-248, 2014.

Patera, R.P., Space Event Detection Method, Journal of Spacecraft and Rockets, 45, 554-559, 2008.

Press, W.H., Flannery, B.P., Teukolsky, S.A., & Vetterling, W.T., Numerical Recipes in C++, 2nd edition, Cambridge University Press, Cambridge, UK, 2002.

Rossi, A., Valsecchi, G., & Alessi, E.M., Evaluation index for the ranking of LEO objects, 65th International Astronautical Congress, Toronto, Canada, IAC-14.A6.2.7, 2014.

Vallado, D., & Seago, J.H., Covariance realism, AAS-AIAA Astrodynamics Specialist Conference, Pittsburgh, USA, 2009.

Vallado, D., & Finkleman, D., A critical assessment of satellite drag and atmospheric density modelling, Acta Astronautica, 95, 141-165, 2014.

White, A.E., & Lewis, H.G., The many futures of active debris removal, Acta Astronautica, 95, 189-197, 2014.